Magnetic X-ray Dichroism in the Spectroscopy of Ultrathin Magnetic Alloy Films

G. Mankey – University of Alabama

et al.

Citation of published version:

Tobin, J., et al. (1996): Magnetic X-ray Dichroism in the Spectroscopy of Ultrathin Magnetic Alloy Films. *Journal of Vacuum Science and Technology B*, 14(4).
DOI: https://doi.org/10.1116/1.588802

Magnetic x-ray dichroism in the spectroscopy of ultrathin magnetic alloy films

J. G. Tobin, K. W. Goodman, G. J. Mankey, R. F. Willis, J. D. Denlinger, E. Rotenberg, and A. Warwick

Citation: Journal of Vacuum Science & Technology B: Microelectronics and Nanometer Structures Processing, Measurement, and Phenomena **14**, 3171 (1996); doi: 10.1116/1.588802

View online: https://doi.org/10.1116/1.588802

View Table of Contents: https://avs.scitation.org/toc/jvn/14/4

Published by the American Institute of Physics

Magnetic x-ray dichroism in the spectroscopy of ultrathin magnetic alloy films

J. G. Tobin[a] and K. W. Goodman
Lawrence Livermore National Laboratory, Livermore, California 94550

G. J. Mankey[b] and R. F. Willis
Physics Department, Pennsylvania State University, University Park, Pennsylvania 16802

J. D. Denlinger, E. Rotenberg, and A. Warwick
Advanced Light Source, Lawrence Berkeley Laboratory, Berkeley, California 94720

(Received 2 October 1996; accepted 6 May 1996)

The magnetic structure of nanoscale alloy films has been probed using the magnetic x-ray linear dichroism in photoelectron spectroscopy and magnetic x-ray circular dichroism in x-ray absorption spectroscopy. FeNi and CoFe epitaxial films were grown on Cu(001), *in situ* and using MBE techniques. Because soft x-rays were used to probe the $2p$ and $3p$ core levels, both elemental selectivity and magnetic sensitivity were achieved simultaneously. Correlation of these magnetic techniques with compositional and structural information will be done. Ultimately, from studies such as this a complete determination of the structure-property relationships will be achievable.

I. INTRODUCTION

A full elucidation of the underlying principles driving magnetic properties in complex systems will require the applications of probes that couple elemental specificity and magnetic sensitivity. Two important classes of magnetic devices, spin valves,[1] and GMR materials[2] are typically composed of several nanoscale layers or aggregations[3] composed of different elements or alloys. The ultrathin nature of these films or clusters further complicates the picture by introducing the impact of interfacial effects, including pseudomorphic strain and spin-specific scattering at the interfaces.[4] One avenue to address such issues is to build epitaxial ultrathin alloy films and probe them directly using techniques that are both elementally selective and magnetically sensitive. Here we report the beginnings of such a study, using CoFe and FeNi films grown with molecular beam epitaxy (MBE) techniques and investigated with magnetic x-ray linear dichroism[5–7] (MXLD) in the core-level photoelectron spectroscopy of the $3p$ states and magnetic x-ray circular dichroism in the x-ray absorption[8] of the $2p$ states (Fig. 1).

II. EXPERIMENT

The x-ray absorption experiments (Fig. 2) were performed at the Stanford Synchrotron Radiation Laboratory (SSRL) using Beamline 8-2, part of the University of California/National Laboratories facilities.[9] Beamline 8-2, is based on a spherical grating monochromator with only three optical elements reflecting the x rays, including the gratings. Extraction of circularly polarized x-rays was achieved by either raising or lowering the first mirror or insertion of vertical slit for blocking part of the beam.[8,10] As illustrated in Fig. 1, in x-ray absorption an electron moves from a core level into the unoccupied density of states immediately above the Fermi energy. The combination of circularly polarized excitation (x rays), strong dipole selection rules, and spin-polarized valence bands (i.e., magnetized atom) gives rise to strong dichroic effects in these spectra, as we will see below. In this experiment, total yield detection was utilized. Here, the cascade of electrons, including Auger decay electrons, but more predominantly low-energy secondary electrons, causes a net loss of electrons by the sample. Hence, we can measure the absorption of ultrathin films simply by monitoring the replenishing current through a picoammeter (A). Because we are using ultrathin films of only multiple monolayer thickness, x-ray attenuation, and electron escape depth effects will be minimized if not totally eliminated. From these intensity variations, and within a localized picture, it is possible to extract, with varying degrees of precision and accuracy, the spin and orbital components of the elemental magnetic moments.[8] For more detail concerning MXCD absorption, please see Ref. 8 and references therein. Sample cleanliness and composition were monitored with photoelectron spectroscopy using photons of about 500 eV for excitation.

The MXLD photoemission measurements (Fig. 3) were made at the Spectromicroscopy Facility (Beamline 7) of the Advanced Light Source at Lawrence Berkeley Laboratory.[11] Extraordinarily bright, linearly polarized x-rays were generated by the U 5.0 undulator and wavelength selection was achieved using the spherical grating monochromator, with a resolving power of over 8000. The photoelectrons were detected using the angle-resolving, multichannel, 5.4 in. radius, Perkin–Elmer hemispherical deflector system. Sample alignment (including pseudomorphic growth), cleanliness, and composition were measured using the hemispherical deflector and a separate Mg $K\alpha$ (photon energy=1254 eV) source, thus freeing up the beamline for other uses during our periods of sample preparation. The actual MXLD measurements

[a]Electronic mail: Tobin1@LLNL.GOV
[b]Present address: Louisiana State University, Physics Department, Baton Rouge, LA 70803.

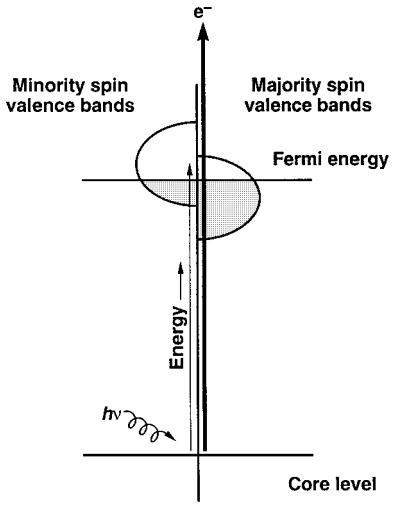

FIG. 1. Shown here is the excitation of a core-level electron in a magnetically polarized atom, i.e., the valence bands are spin polarized. For illustrative purposes only, a circularly polarized photon is shown, with a minority electron moving into the unoccupied valence (conduction) band and a majority electron being ejected. In x-ray absorption (light vertical arrow) near-edge measurements, the electron moves into the strongly polarized valence states (e.g., the $3d$ states), giving rise to strong dichroic effects at the $l+\frac{1}{2}$ and $l-\frac{1}{2}$ edges. In photoelectron spectroscopy (heavy vertical arrow with e^-), the electron moves into states well above the strongly polarized conduction bands and is collected in an energy analyzer.

used the highly linearly polarized synchrotron radiation and were performed with a total instrumental energy resolution of less than 100 meV and angular resolution of 2° or less. The angle of incidence of the x rays was 30° relative to the surface plane. The electrons were collected along the surface normal; i.e., ''normal emission.'' Typically, the magnetic alloy was magnetized in the plane of the surface but perpendicularly to the plane containing the emission direction (surface normal) and the Poynting vector and electric polarization vector of the x rays. Thus, the ''transverse-chiral'' condition necessary for MXLD was achieved: reversing the magnetic field causes two mirror-image configurations that are equivalent but totally nonsuperimpossible. By comparing spectra from these configurations, it is possible to directly probe the magnetic perturbations of the elementally specific electronic structure of the systems.

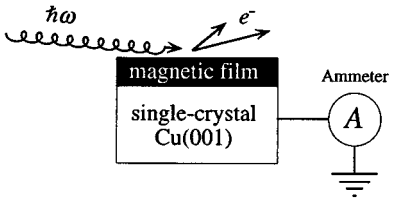

FIG. 2. Shown here is a schematic representation of the MXCD absorption experiment. A total yield method has been used. The picoammeter (A) monitors the grounding current, giving a measure of the absorption in an ultrathin film. It is necessary to align and antialign the magnetization and helicity or circular polarization, hence grazing incidence (15°) is used with in-plane magnetized samples (see Ref. 8).

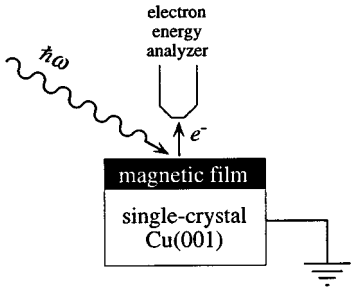

FIG. 3. The MXLD experimental configuration is schematically shown here. The grazing angle of incidence of the linearly polarized x rays was 30°, relative to the surface plane. Electrons ejected perpendicularly to the surface were collected by the angle resolving detector (i.e., normal emission). The plane containing the ejected electron and the Poynting vector of the x ray also contained the electric (linear polarization) vector of the x ray as well. The magnetization vector was perpendicular to this experimental plane, but in the plane of the surface. To achieve MXLD, comparisons were made between spectra in which only the direction of the magnetization was reversed; all else was kept the same.

III. OVERLAYER GROWTH: COMPOSITION, THICKNESS, AND ORDERING

The alloy systems under consideration were CoFe and FeNi. Ultrathin films of each were grown on Cu(001) at room temperature, using well-developed MBE techniques.[12] All samples were about 2–5 monolayers thick. Studies of the bulk electronic structure have been performed,[13–16] but the properties of these pseudomorphic overlayers are further complicated by epitaxial strain and other nanoscale effects. An important issue is growth control, including thickness, composition, and ordering. At the ALS,[11] we can monitor thickness and composition by performing x-ray photoelectron spectroscopy (XPS) and element specific ordering with x-ray photoelectron diffraction (XPD), using the Mg $K\alpha$ x-ray source. Examples of XPS spectra are shown in Fig. 4. The XPD analyses are illustrated in Figs. 5 and 6.

Figure 4 illustrates the type of quantitative information that can be gleaned from XPS. Here, three major sets of peak structure are immediately apparent: The Cu $2p$ ($B^F=933$, 952 eV), the Co $2p$ ($B^F=778$, 793 eV), and the Fe $3p$ ($B^F=707$, 720 eV) (B^F is the binding energy with respect to the Fermi level.) The relative intensities of the Fe and Co lines give a zeroth order estimate of composition, assuming chemical disorder within the alloy overlayer. The relative intensity of the Cu $2p$ lines versus the sum of the Co and Fe lines gives a measure of overlayer thickness, if there is no substrate intermixing or other such complications. A quantitative estimate of thickness requires assumptions concerning x-ray penetration depths and electron escape depths. Quantitative estimates in general necessitate corrections for photon energy dependent cross sections and angles of emission. After properly including such effects, it is possible to arrive at composition and thickness estimates such as those shown in Fig. 4.

A key question in the growth of epitaxial films is that of the degree and nature of ordering, including strain. A means to probe ordering in ultrathin films in an elementally specific

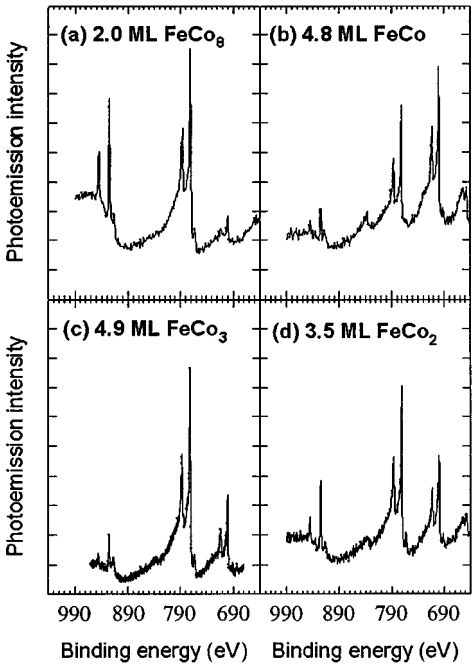

FIG. 4. XPS analysis of various Fe$(1-x)$ Co(x) alloy overlayers on Cu(001). Spectral structure includes the Fe $2p$ ($B^F=707$, 720 eV), Co $2p$ ($B^F=778$, 793 eV) and Cu $2p$ ($B^F=932$, 952 eV). The sample in (c) may be slightly Fe rich at the interface; this effect was not included in the concentration estimate.

fashion is the application of forward focusing in x-ray photoelectron diffraction (XPD).[17–19] Here, buried atoms emit core-level photoelectrons when excited with x rays and intensity maxima correspond to positions of nearby atoms

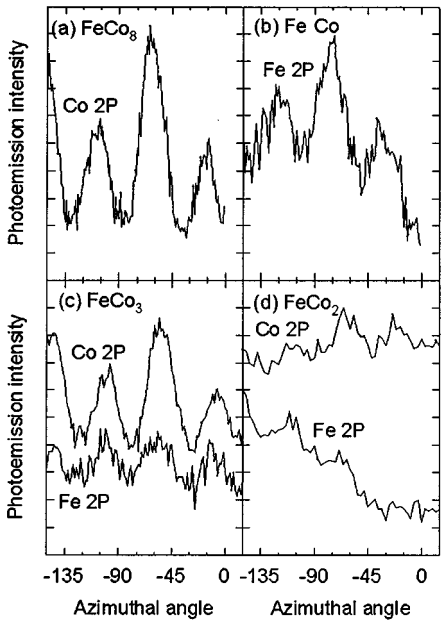

FIG. 5. XPD azimuthal scans are shown here, for a series of FeCo alloy overlayers, with the energy set to the core levels of either Co or Fe. The polar angle is 45°: the diffraction peaks demonstrate the degree to which the overlayer atoms are occupying ordered lattice sites.

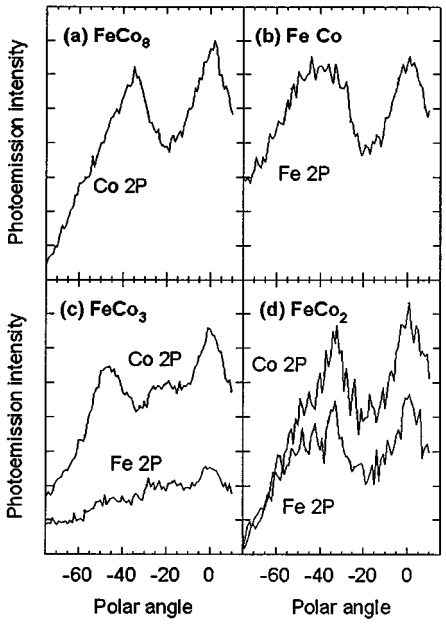

FIG. 6. XPD polar scans are plotted in this figure. The azimuth is set on a peak and the polar angle is scanned. For a, b, and d, the plane of rotation is a {110} plane. For c, it is a {100} plane.

above the emitters. This is because these nearby atoms can act as lenses to focus electrons of fairly high kinetic energies (hundreds of eV or more). Thus, one can immediately identify bond axes or nearest neighbor directions. Of course, complications exist: long chains of atoms can cause defocusing, multiple scattering events can arise, and bulk signals can overwhelm those of a near surface atom of the same elemental nature as the bulk. However, many of these complications are minimized in ultrathin overlayers. In fact, the elemental specificity of the source core level electrons allows for a separation of overlayer (here, Co and Fe) forward focusing from the bulk (Cu) effects and a separation of overlayer components from each other (e.g., Co vs Fe). Thus on can directly probe *overlayer* ordering on an element-by-element basis, independent of substrate ordering effects.

In FeCo alloy films, it is expected that the growth will be FCC-like with the Cu(001) serving as a template. Two tests of this ordering are shown: in Fig. 5 are azimuthal scans and in Fig. 6 are polar scans. FCC growth will give rise to strong forward focusing peaks at a 45° polar angle relative to the normal (0°): this is along the ⟨101⟩ and ⟨011⟩ directions (i.e., the face diagonal). Because of the width of the forward focusing peaks, at 45° polar angle one may also observe part of the ⟨112⟩ and ⟨111⟩ families of peaks, centered at a polar angle of 35° and 55° from the normal (0°), respectively. Thus, an azimuthal scan (polar angle of 45°) will give rise to a series of peaks separated by 45° azimuthally, but possibly with an intensity period of 90° azimuthally. That is what is observed for $FeCo_8$, FeCo, and $FeCo_3$ in Fig. 5, indicating a high degree of ordering. The $FeCo_2$ seems to be more disordered, with only weaker maxima. While a high degree of ordering is indicated, it still needs to be proven that it is

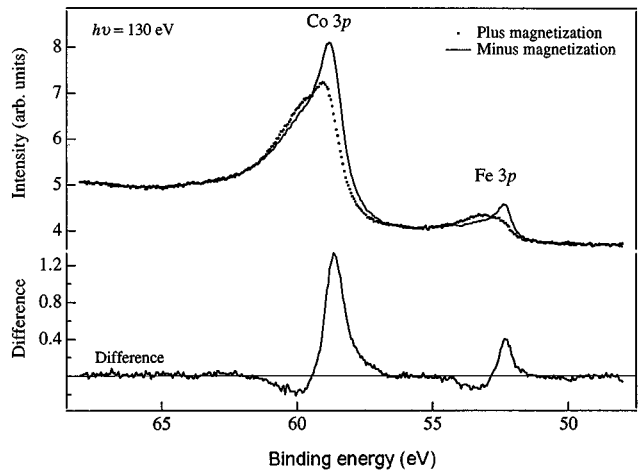

FIG. 7. Photoelectron spectra of 2 ML (Fe[1]Co[9])Cu(001), taken using a photon energy of 130 eV. Also shown is the difference for these two spectra, a measure of the MXLD effect.

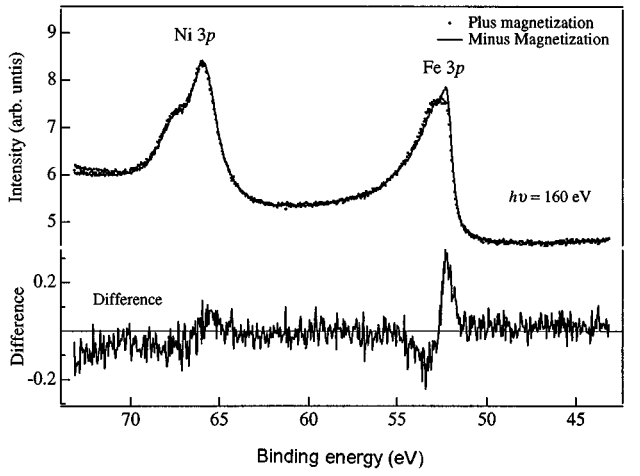

FIG. 8. Photoelectron spectra of 2 ML (Fe[1]Ni[4])Cu(001), taken using a photon energy of 160 eV. Again, a difference spectrum is also shown, as a measure of the MXLD effect.

FCC-like. Unfortunately, BCC growth could give rise to a similar azimuthal pattern, at least qualitatively. A further test of FCC growth is to perform polar scans in the {100} and {110} planes. In the {100} plane, the maximum associated with the ⟨101⟩ should be at 45°: An example of this result is shown in Fig. 6(c). In the {110} plane, the ⟨112⟩ maximum should be at 35° and the ⟨111⟩ maximum at 55°. Figures 6(a), 6(b), and 6(d) show examples of peaks at or near 35°, with possible shoulders at 55°. Normal emission peaks (0°) are also expected and evident in all of the subsections of Fig. 6. In the case of $FeCo_3$ [Fig. 6(c)], the order appears to be stronger around the Co emitters than the Fe emitters, consistent with Fig. 5(c). A complete analysis would, of course, include a full computational simulation and explanation of all features and effects. Nevertheless, the presence of strong maxima indicates a high degree of FCC ordering. It should be noted that while strong structural ordering is indicated here and the source of the photoelectrons can be specified elementally, the scattering events do not have such elemental specificity. Moreover, we assume that while these films are structurally ordered they are chemically disordered, a natural by-product of the simultaneous co-evaporation of Fe and Co onto Cu(001).

IV. MAGNETIC X-RAY DICHROISM

Now, let us turn our attention to the MXLD results. Examples of our spectroscopic MXLD photoemission results are shown in Figs. 7 and 8. In this energy regime, the cross sections for the Fe, Co, and Ni 3P are strongly photon-energy dependent: hence, the peaks do not scale with concentration without further correction. Along with the photo emission spectra are difference curves. From these we can calculate an asymmetry, using the definition $\mathrm{ASYM}=(I^+-I^-)/(I^++I^-)$. Setting each prepeak region equal to zero, asymmetry values of approximately 15% for Co and 40% for Fe in FeCo and 5% for Fe and 2% for Ni in NiFe are obtained.

Presently, we are pursuing studies of these systems where we vary the thickness and composition of the magnetic overlayers and probe the $3p$ levels of each element. In essence, we are attempting to use the MXLD measurements as element-specific, surface magnetometers. This is not quite as straightforward as it might seem: it is clear that simple perturbative (Fig. 9) models often fail.[20,21] For example, if it is possible to work in the regime where $\Delta E_{\mathrm{s.o.}}$, the spin orbit splitting, is large versus ΔE_{EX}, the exchange splitting, then ΔE_{EX} can be treated as perturbation upon $\Delta E_{\mathrm{s.o.}}$. Under these conditions, it seems possible that the variations in asymmetry will correlate with the elemental magnetic moment. A fair candidate for this condition is Ni, where the stronger spin-orbit splitting is evidenced by the peak and shoulder appearance in both spectra in Fig. 8. Fe and Co are probably more difficult cases, where the exchange and spin orbit splittings need to be dealt with on an equal footing, in a non-perturbative approach.[20] However, it may be possible to follow variations around a central value in a perturbative

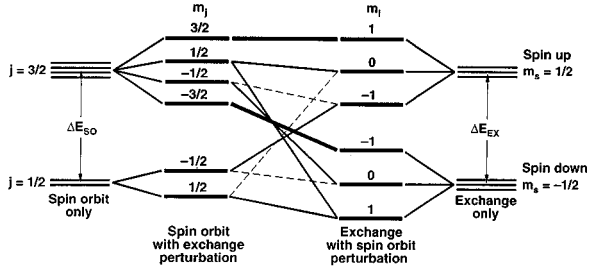

FIG. 9. The effect of spin orbit and exchange splitting upon a p core level is illustrated here. Two perturbative approaches are shown: large spin orbit and small exchange splitting (left) and small spin orbit and large exchange splitting (right). The Ni $3p$ would fall to the left while the Fe $3p$ is near the center, where spin orbit and exchange effects are nearly equal and a non-perturbative approach is required. State mixing is indicated by dashed and solid lines.

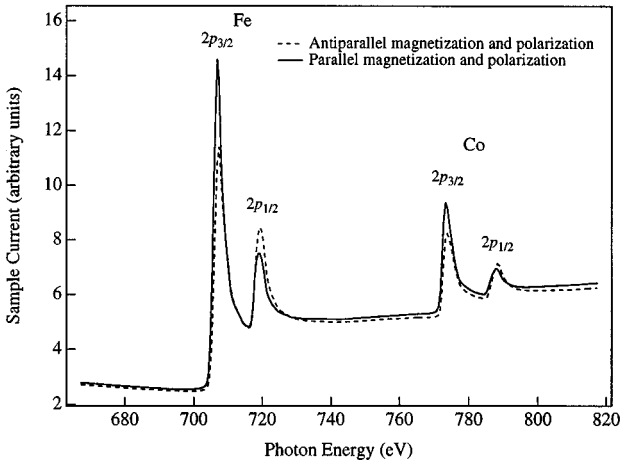

FIG. 10. An example of MXCD absorption is shown here. The 5 ML $(Fe_3Co_1)Cu(001)$ sample was magnetized in-plane. The degree of circular polarization was approximately 70%. This lower-than-usual value was chosen for ease of operation and enhanced counting rates. Corrections for nonideal polarization (<100%) can be made following Ref. 8. Regardless, strong dichroisms are easily observable here.

fashion.[7] Moreover, we can correlate the MXLD photoemission by comparing that technique with the results from MXCD absorption. An example of our MXCD absorption results is shown in Fig. 10. Here, a strong dichroism is observed at both the Fe $2p$ and Co $2p$ peaks. Within certain limitations,[8] it is possible to extract from such spectra both the spin and orbital components of the projection of the elementally specific magnetic moments along the axis of quantization. (Again, it should be noted that the ultrathin nature of our samples minimizes the impact of electron escape or x-ray attenuation effects.) Although our initial results are only preliminary and further study is warranted, they are promising in terms of understanding key effects in magnetic nanoscale films, including such possibilities as strain-modified invar quenching.

V. SUMMARY

We are using the elementally specific and magnetically sensitive techniques of MXLD photoelectron spectroscopy and MXCD absorption to probe the structure-property relationships of nanoscale magnetic alloys. These ultrathin films are the building blocks of many new magnetic devices, including spin-valve and GMR materials. The variation of classical magnetic effects, such as invar quenching, due to pseudomorphic strain and other nanoscale perturbations, is being investigated.

ACKNOWLEDGMENTS

This work was performed under the auspices of the U.S. Department of Energy by the Lawrence Livermore National Laboratory under Contract No. W-7405-ENG-48. The Spectromicroscopy Facility and the Advanced Light Source were constructed with support from the U.S. Department of Energy. The ALS and SSRL are operated under support from the U.S. Department of Energy.

[1]B. A. Gurney, V. S. Speriosu, J. P. Nozieres, H. F. Lefakis, D. R. Wilhoit, and D. U. Need, Phys. Rev. Lett. **71**, 4023 (1993); B. Dieny, V. S. Speriosu, S. Metin, S. S. P. Parkin, B. A. Gurney, P. Baumgart, and D. R. Wilhoit, J. Appl. Phys. **69**, 4774 (1991); B. Dieny, V. S. Speriosu, S. S. P. Parkin, B. A. Gurney, D. R. Wilhoit, and D. Mauri, Phys. Rev. B **43**, 1297 (1991).
[2]S. S. P. Parkin, Phys. Rev. Lett. **71**, 1641 (1993); A. C. Ehrlich, Phys. Rev. Lett. **71**, 2300 (1993); V. Grolier *et al.*, Phys. Rev. Lett. **71**, 3023 (1993).
[3]R. Marks *et al.*, Mater. Res. Soc. Symp. Proc. **313**, 411 (1993).
[4]N. M. Rensing and B. M. Clemens, Mater. Res. Soc. Symp. Proc. **313**, 197 (1993); J. M. George *et al.*, Mater. Res. Soc. Symp. Proc. **313**, 737 (1993).
[5]C. H. Roth, F. U. Hillebrecht, H. B. Rose, and E. Kisker, Phys. Rev. Lett. **70**, 3479 (1993); Solid State Commun. **86**, 647 (1993).
[6]W. Kuch, M. T. Lin, W. Steinhogl, C. M. Schneider, D. Venus, and J. Kirschner, Phys. Rev. B **51**, 609 (1995).
[7]G. Rossi, F. Sirotti, N. A. Cherepkov, F. Cambet-Farnoux, and G. Panaccione, Solid State Commun. **90**, 557 (1994); F. Sirotti and G. Rossi, Phys. Rev. B **49**, 15682 (1994).
[8]J. G. Tobin, G. D. Waddill, A. F. Jankowski, P. A. Sterne, and D. P. Pappas, Phys. Rev. B **52**, 6530 (1995).
[9]K. G. Tirsell and J. Karpenko, Nucl. Intrum. Methods A **291**, 511 (1990).
[10]L. J. Terminello, G. D. Waddill, and J. G. Tobin, Nucl. Instrum. Methods A **317**, 271 (1992).
[11]J. D. Denlinger, E. Rotenberg, T. Warwick, G. Visser, J. Nordgren, J. H. Guo, P. Skytt, S. D. Kevan, K. S. McCutcheon, D. Shuh, J. Bucher, N. Edelstein, J. G. Tobin, and B. P. Tonner, Rev. Sci. Instrum. **66**, 1342 (1995).
[12]G. J. Mankey, M. T. Kief, and R. F. Willis, J. Vac. Sci. Technol. A **9**, 1595 (1991); F. Huang, M. T. Kief, G. J. Mankey, and R. F. Willis, Phys. Rev. B **49**, 3962 (1994).
[13]D. D. Johnson, F. J. Pinski, and J. B. Staunton, J. Appl. Phys. **61**, 3715 (1987).
[14]I. A. Abrikosov, O. Eriksson, P. Soderlind, H. L. Skiver, and B. Johansson, Phys. Rev. B **51**, 1058 (1995).
[15]P. Soderlind, O. Eriksson, B. Johansson, R. C. Albers, and A. M. Boring, Phys. Rev. B **45**, 12911 (1992).
[16]C. Kittel, *Introduction to Solid State Physics*, 6th ed. (Wiley, New York, 1953), p. 437.
[17]W. F. Egelhoff, Jr., Phys. Rev. B **30**, 1052 (1984).
[18]S. A. Chambers, T. J. Wagener, and J. H. Weaver, Phys. Rev. B **36**, 8992 (1987).
[19]H. C. Poon and S. Y. Tong, Phys. Rev. B **30**, 6211 (1984).
[20]E. Tamura, G. D. Waddill, J. G. Tobin, and P. A. Sterne, Phys. Rev. Lett. **63**, 3642 (1992).
[21]J. G. Tobin, G. D. Waddill, E. Tamura, P. A. Sterne, P. J. Bedrossian, X. Guo, and S. Y. Tong, Surf. Rev. Lett. (in press).